The Abdus Salam
International Centre for Theoretical Physics

United Nations
Educational, Scientific and
Cultural Organization

IAEA
International Atomic Energy Agency

2137-16

Joint ICTP-IAEA Advanced Workshop on Multi-Scale Modelling for Characterization and Basic Understanding of Radiation Damage Mechanisms in Materials

12 - 23 April 2010

Effects of Pulsed Irradiation: Assessment of the problem and some Multiscale Modeling

J.M. Perlado
Universidad Politecnica de Madrid
Spain

Strada Costiera 11, 34151 Trieste, Italy - Tel.+39 040 2240 111; Fax +39 040 224 163 - sci_info@ictp.it

Effects of Pulsed Irradiation: Assessment of the problem and some Multiscale Modeling

J.M. Perlado

Instituto Fusion Nuclear

Universidad Politécnica de Madrid

Inertial Confinement Fusion

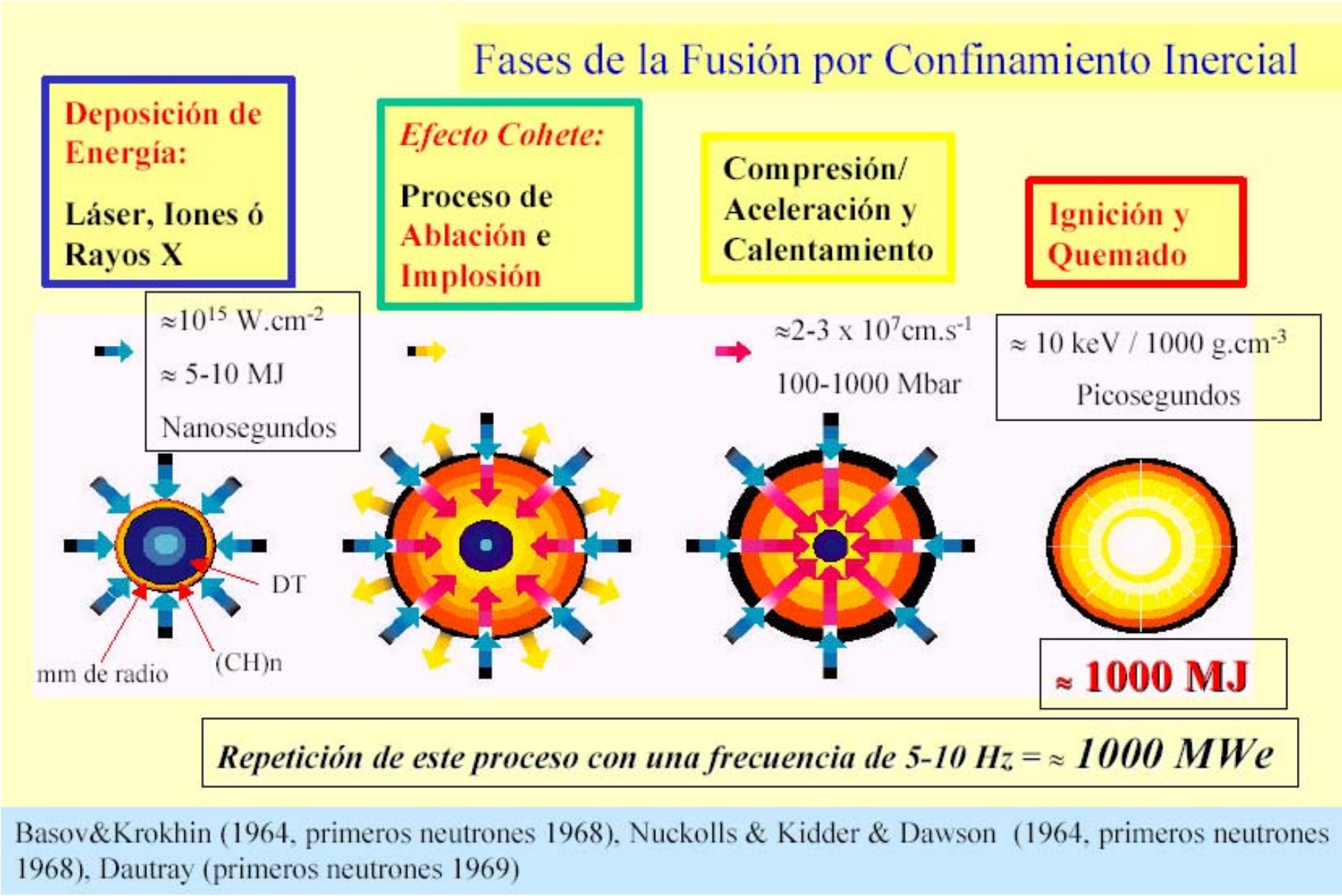

Basov&Krokhin (1964, primeros neutrones 1968), Nuckolls & Kidder & Dawson (1964, primeros neutrones 1968), Dautray (primeros neutrones 1969)

The National Ignition Facility concentrates all the energy in a football stadium-sized facility into a mm^3

The National Ignition Facility

Láser de Nd Cristal con Energía de 1.8 MJ en 3w (=0.35 μm) con 192 haces y que dará una ganancia energética de 30 como máximo (E por fusión/E de iluminación del blanco por el láser)

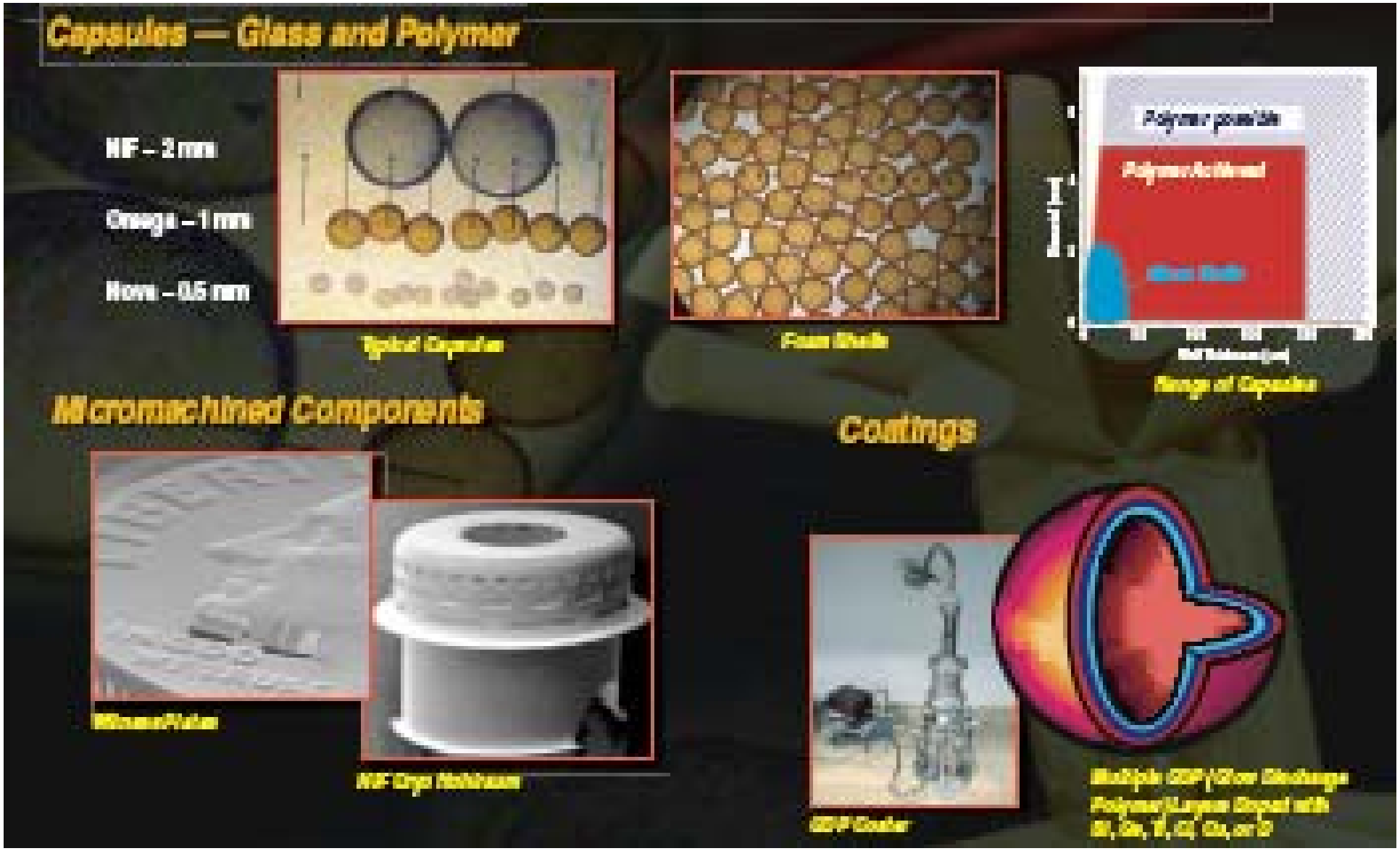
Capsules — Glass and Polymer
NF – 2 mm
Omega – 1 mm
Hovo – 0.5 mm
Micromachined Components
Coatings

movie

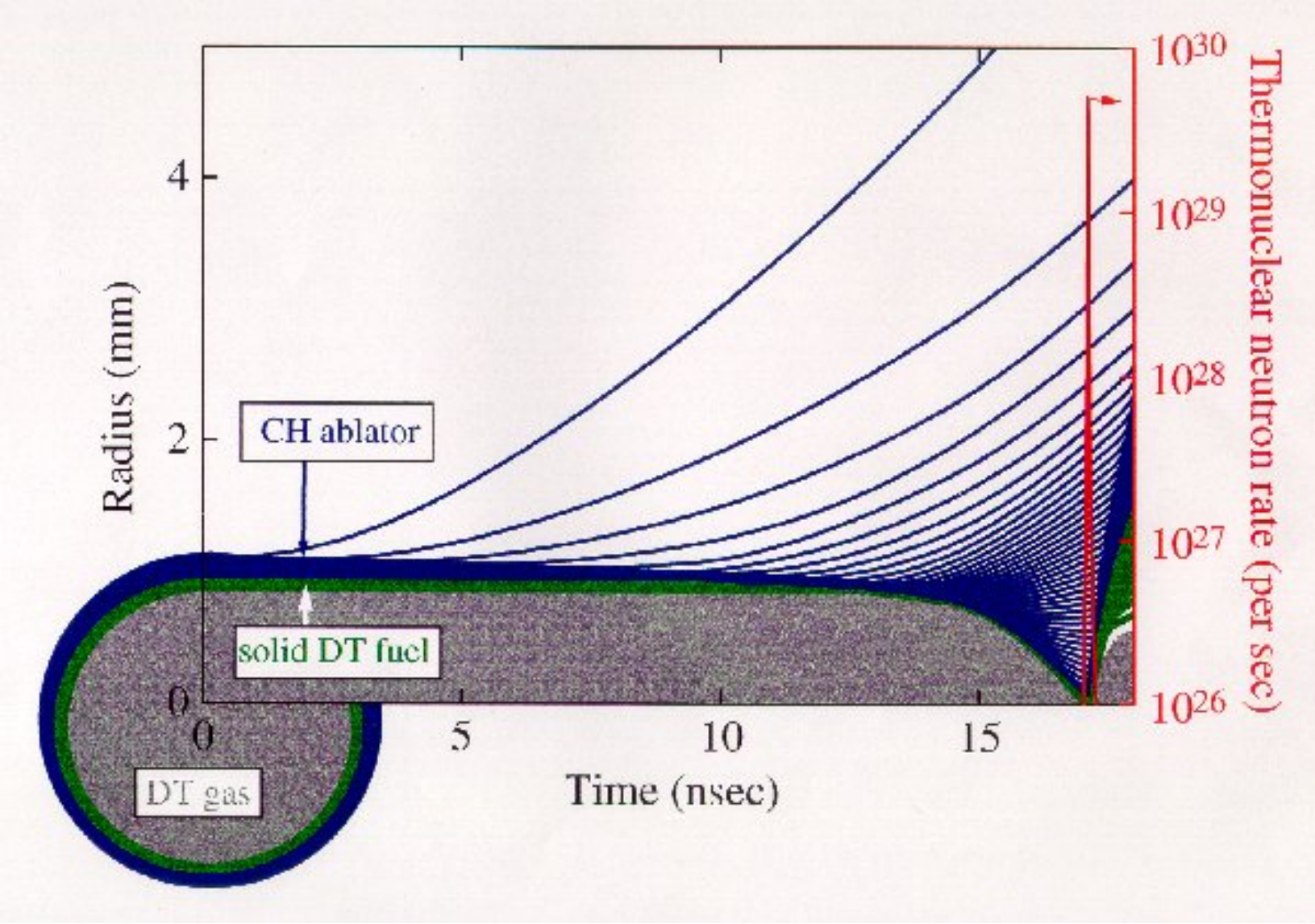
Radius (mm)
4
2
0
0
5
10
15
Time (nsec)
CH ablator
solid DT fuel
DT gas
10^{30}
10^{29}
10^{28}
10^{27}
10^{26}
Thermonuclear neutron rate (per sec)

Neutron Spectra High gain capsule with

<> 2x 10^{20} neutrons / pulse

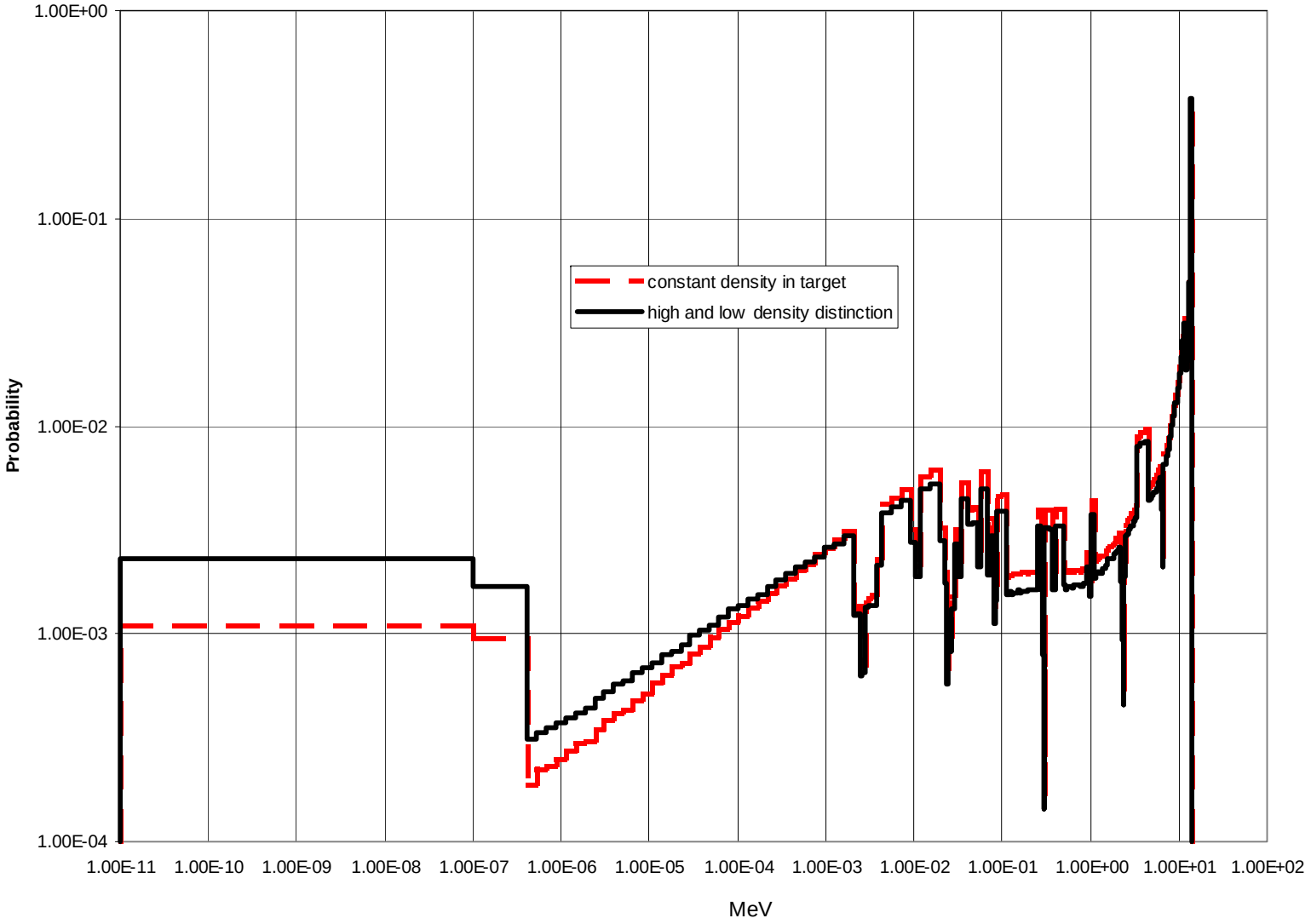

Inertial Confinement Fusion: Reactor concepts and NIF MATERIALS assessment

HYLIFE-II

Type of Facility:

Ignition, Reactor/Protection

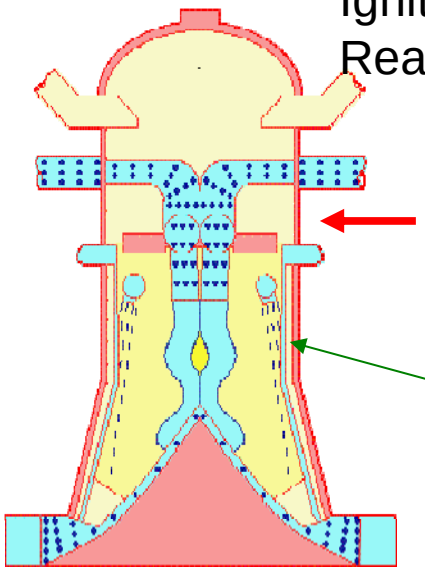

- **Structural Material :** Steel SS304 Lifetime = that of the plant
- **Flibe:** Coolant, T reproduction, and protection

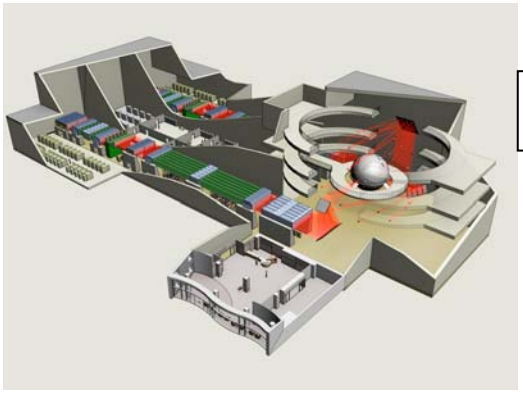

HiPER

MATERIALS

Target composition

(nanostructures)

First Wall, **Optics**

Structural, **Coolant**

Activation and Damage

Heat Deposition, T economy

Effects of:

Neutron

Debris

Shrapnel

X-rays; High T; High P

NIF

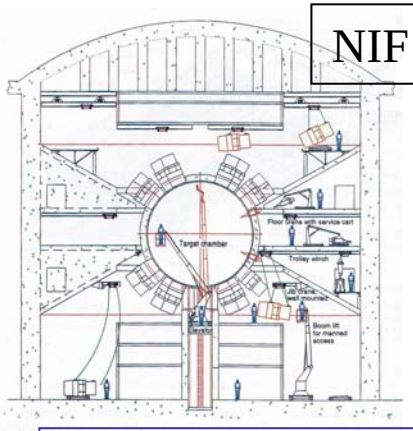

SOMBRERO

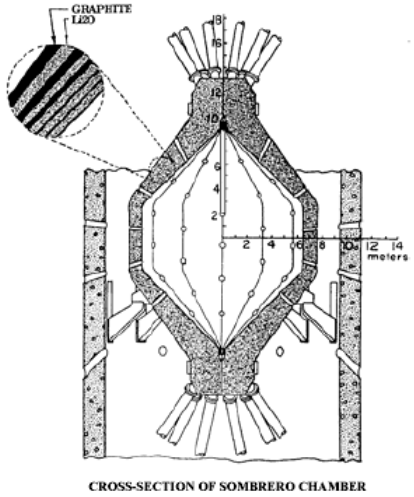

CROSS-SECTION OF SOMBRERO CHAMBER

IFE REACTORS DESIGNS

Table 1.1: Comparison of main parameters of past IFE reactor designs with FALCON-D (the reactor designed in this study).

	KOYO	KOYO-Fast	HAPL	FALCON-D
chamber radius [m]	4	3	11	5~6
ignition method	central ignition	fast ignition	central ignition	fast ignition
chamber wall	liquid wall		dry wall*1	dry wall
injection energy E_{in}[MJ] (implosion / heating)	3.4	1.2 (1.13/0.07)	2.36*2	0.4 (0.35/0.05)
pellet gain G	176	167	148	100
target yield E_{fus}[MJ]	600	200	350	40
wall load (except neutron) [J/cm2]	60	35	4.6	~ 2.0
repetition rate f_{rep}[Hz]	12(3 × 4)	16(4 × 4)	5	30
fusion output P_{fus}[MW]	7200	3200	1750	1200

*1 Also considering the magnetic intervention method [9] .
*2 Not found in the reference; calculated from the fusion gain and target yield.

MAIN THREATS TO THE CHAMBER WALL
-High temperatures -> evaporation
-Ion implantation (in particular He)
-Sputtering, ablation
-Mechanical damage (roughening, embrittlement,…)
-Neutrons

NEUTRONICS 3D DETAILED CALCULATIONS USING CAD AND MCNPX. It is time to start to use in Inertial Fusion Reactors Concepts and Facilities to get consequences such as Activation / Damage …….defining structures and materials……

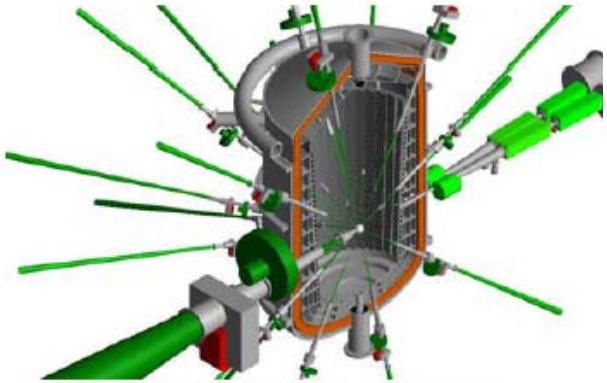

Figure 1: KOYO-F modular reactor.

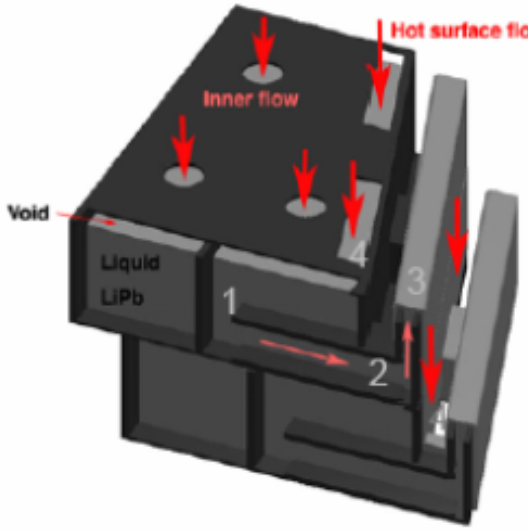

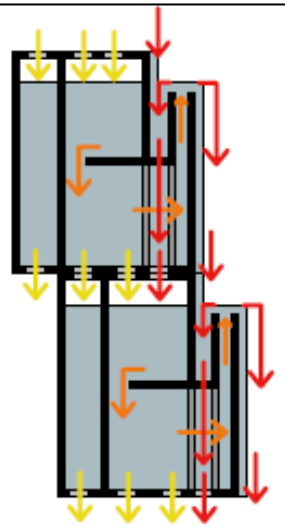

Figure 2: KOYO-F blanket inner loop

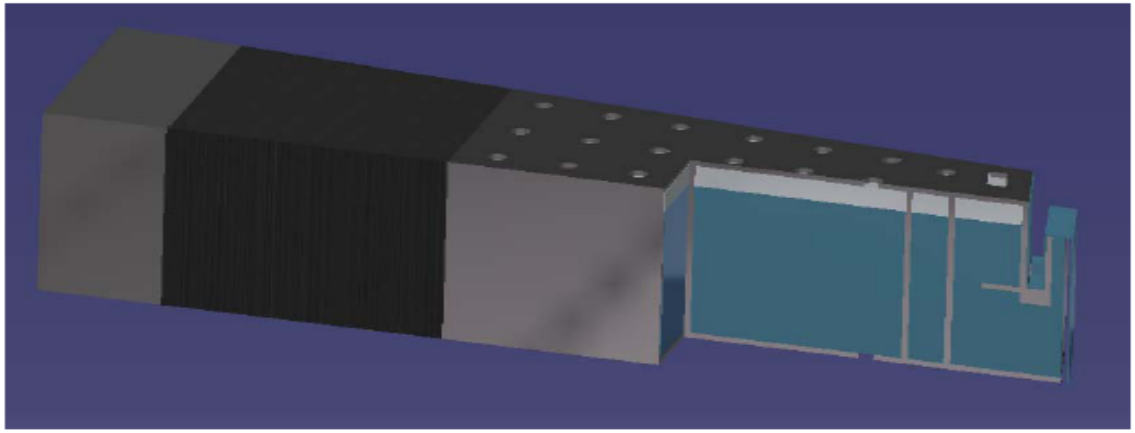

Figure 3: KOYO-F blanket CAD modeling.

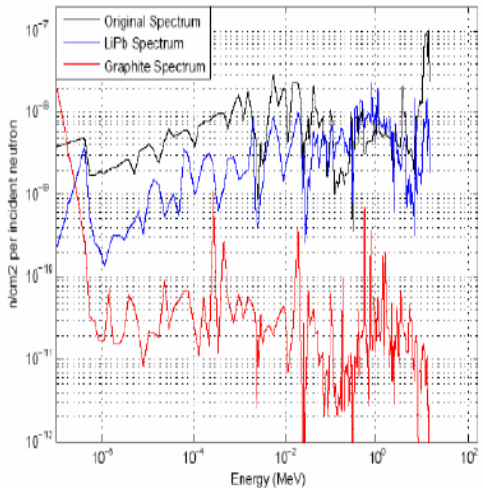

3 April 2010

Duration of the pulse in the wall

According to transport calculation

130 ns from 14 MeV unscattered neutron

Assuming 4 m Radius

-ASSUMING TARGET SPECTRAL CONDITIONS

- PROTECTED (66 CM) WALL

Wall after protection = 1 cm of Fe

DAMAGE RATE

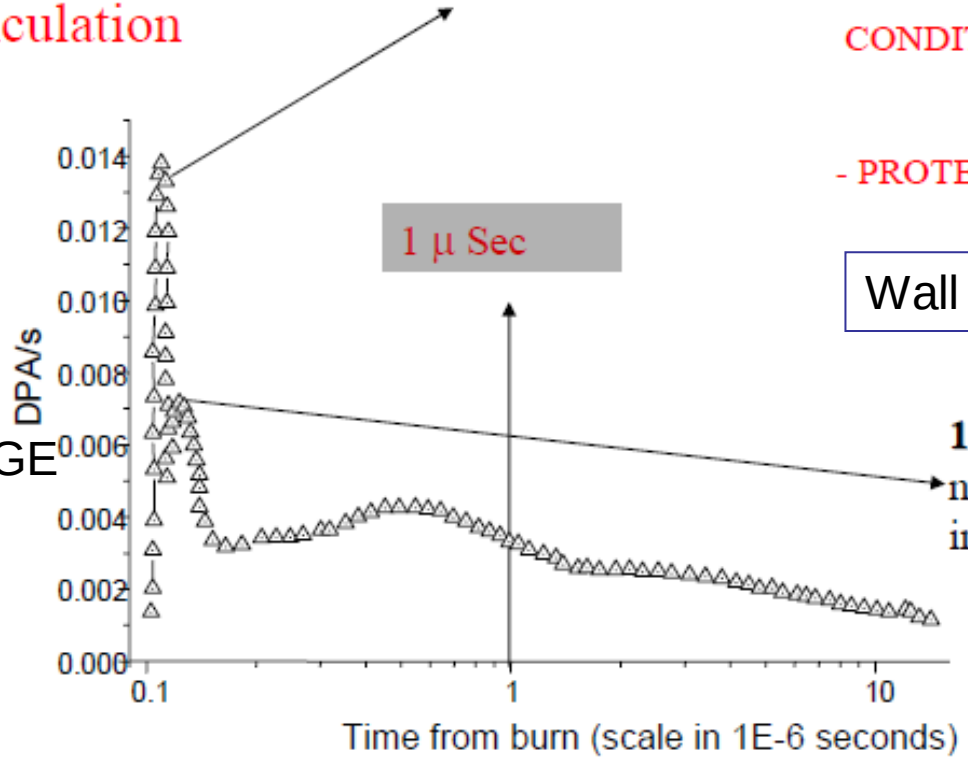

170 ns from neutrons scattered in the blanket

MonteCarlo detailed calculations

Effects of

Protection started a long time ago to be studied.

Under specific design NEW STUDIES ARE NEEDED

NECESSITY OF CFD codes !!!!!!!!

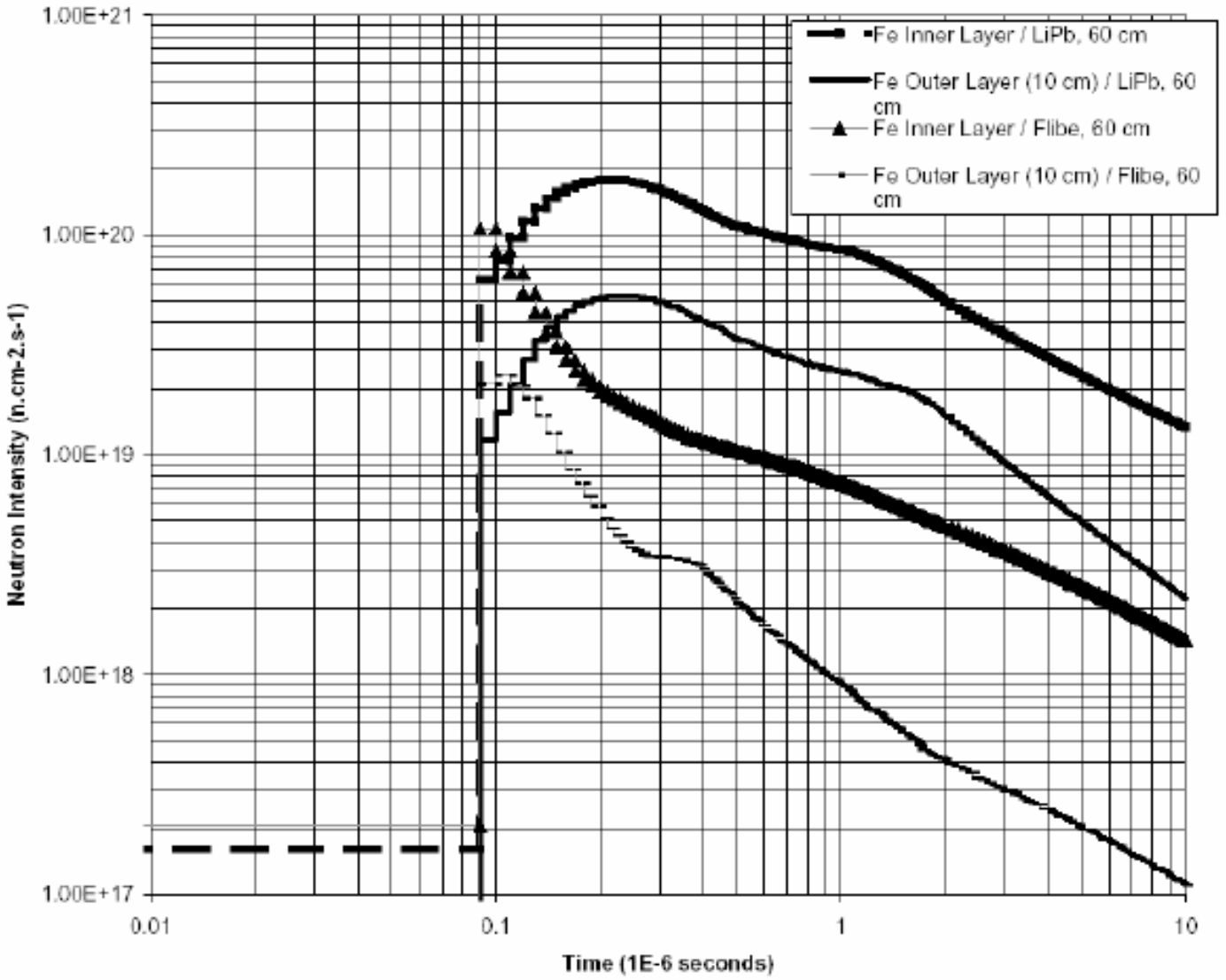

Neutron Intensity versus Time after Target Emission (μs) for Inner and Outer Fe layers (thickness 10 cm) and LiPb and Flibe protections (60 cm).

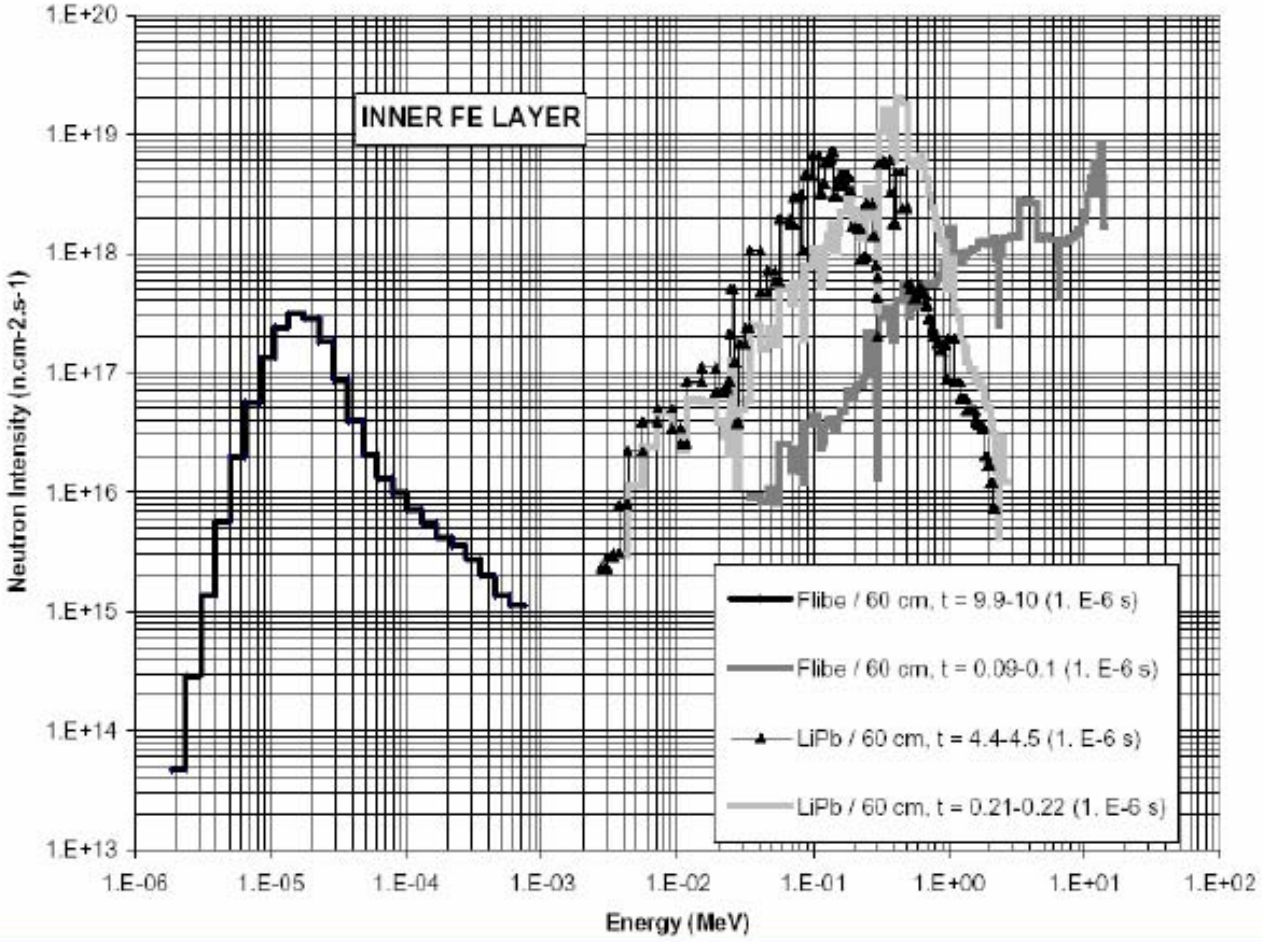

Neutron Spectra in the Inner Fe Layer for LiPb and Flibe protections in the time of Neutron Maximum Intensity and later in the temporal evolution.

Time dependent neutronics in IFE pulsed emissions in structural materials

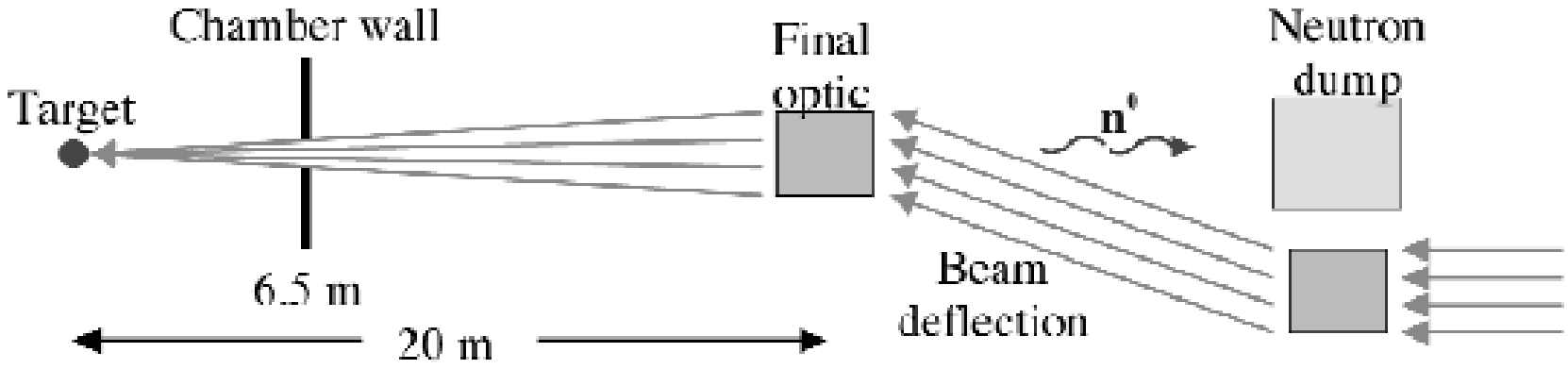

Incoming laser is first deflected and focused in the final optics

Chamber wall positioned radially between target and optics with penetrations to allow the entry

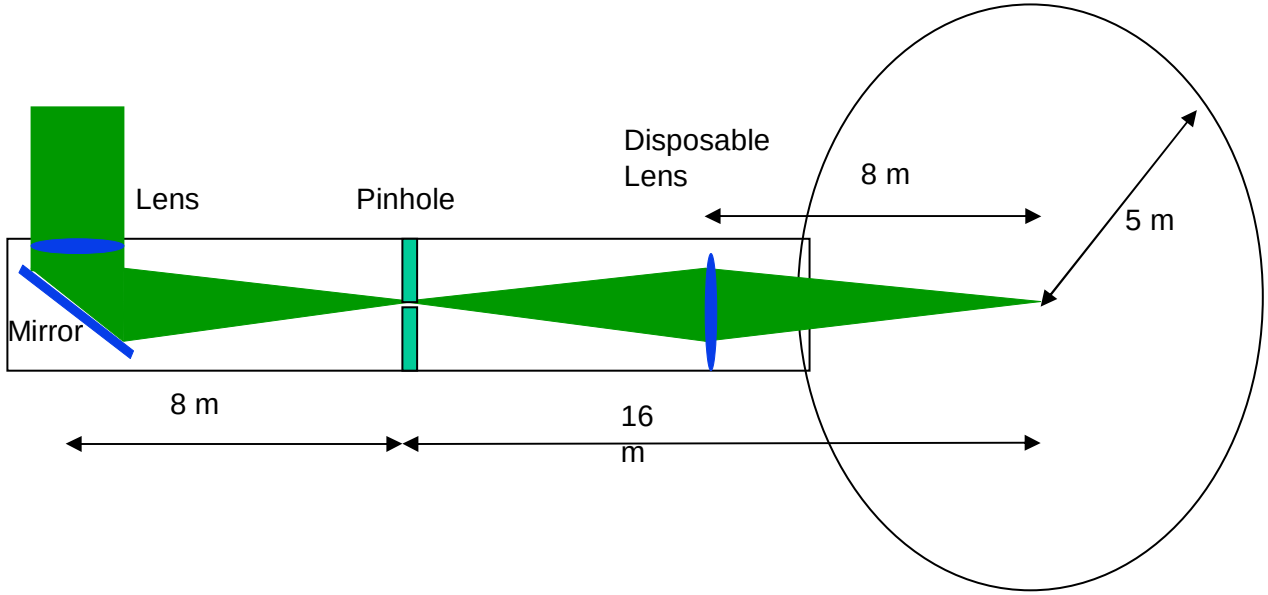

- High energy neutrons
- X-Rays
- Chamber black body like radiation
- Ion debris

Neutron production Scaling depending on laser energy

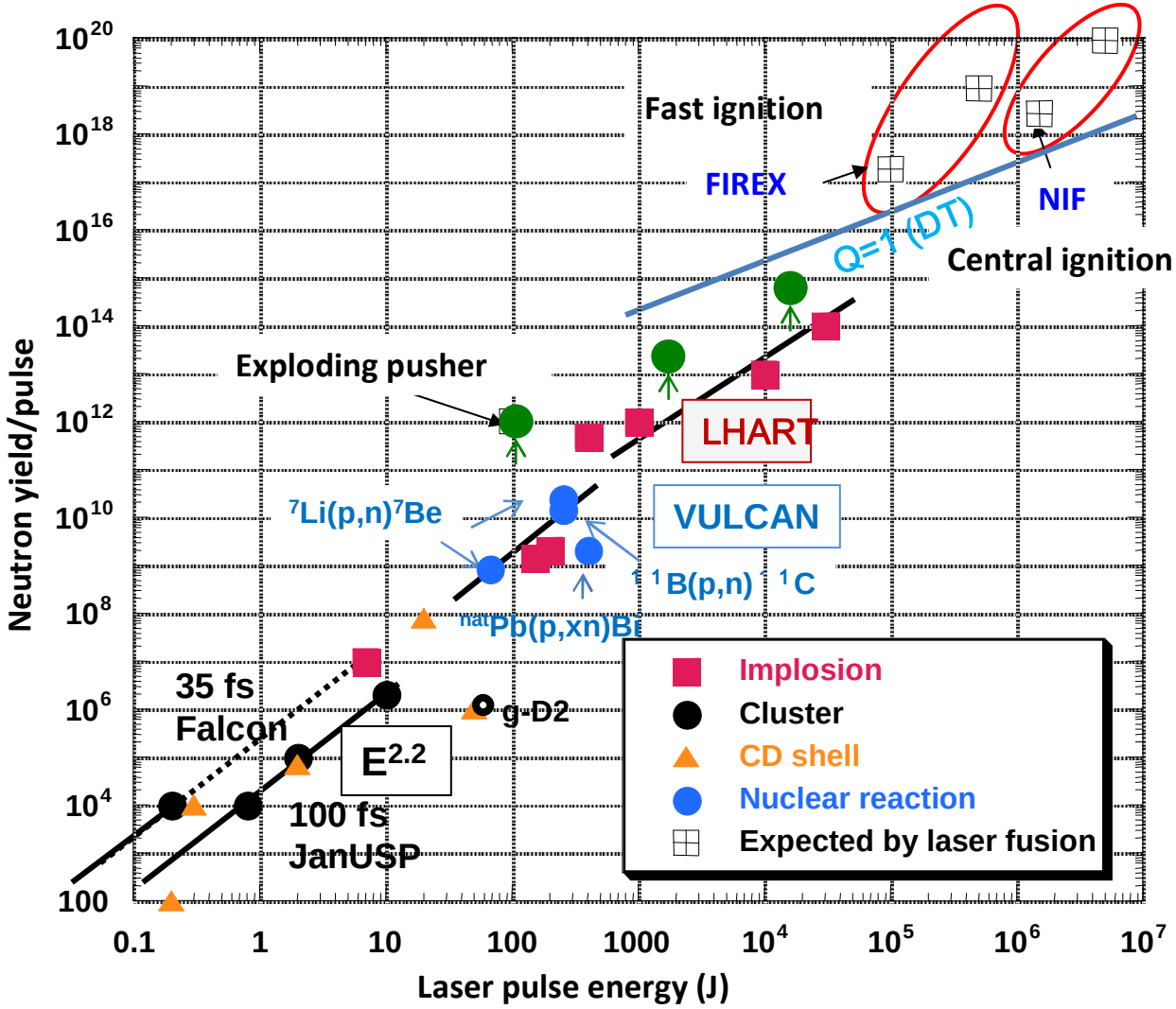

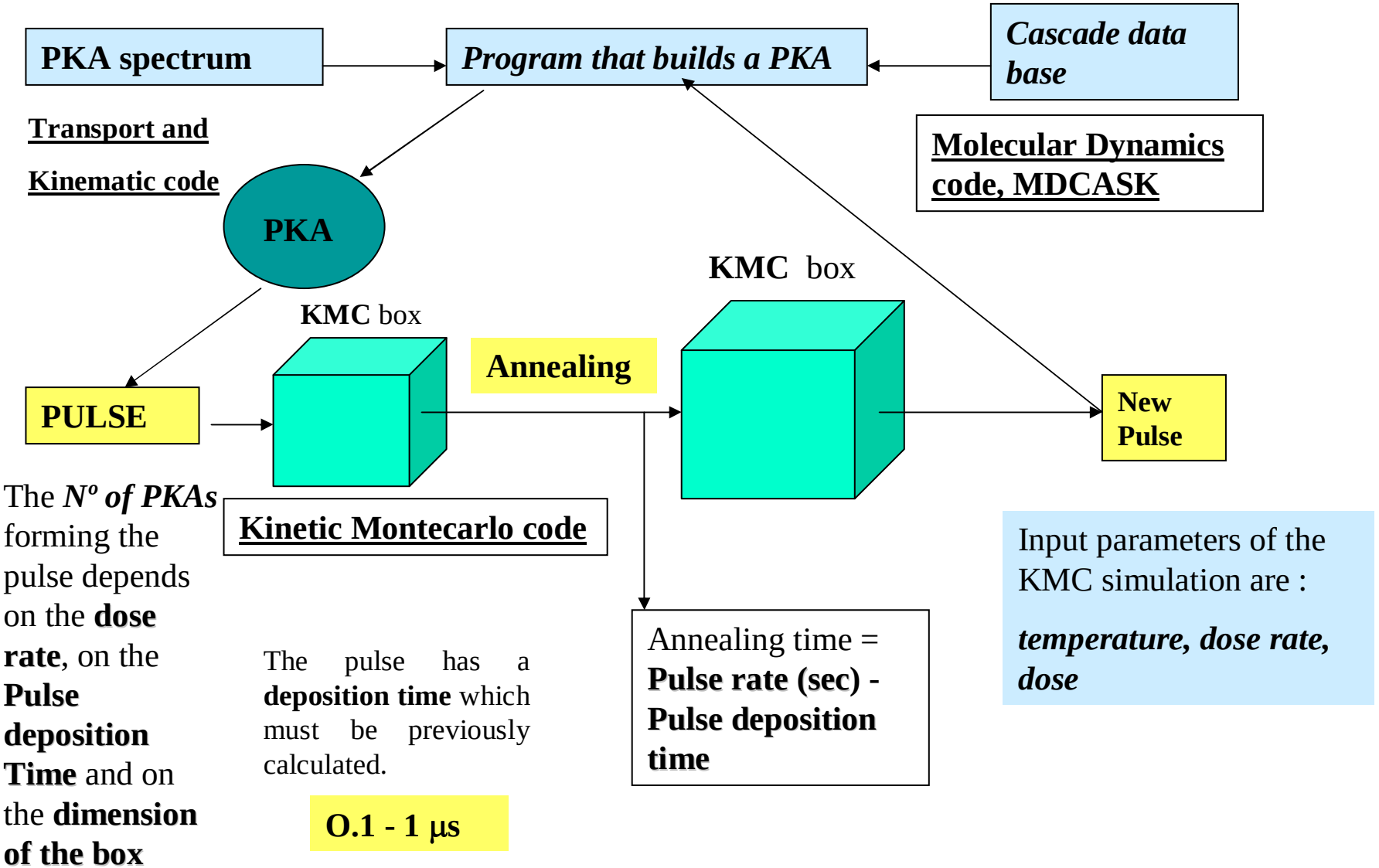
PKA spectrum
Program that builds a PKA
Cascade data base
Transport and
Kinematic code
Molecular Dynamics code, MDCASK
PKA
KMC box
KMC box
Annealing
PULSE
New Pulse
Kinetic Montecarlo code
The Nº of PKAs forming the pulse depends on the dose rate, on the Pulse deposition Time and on the dimension of the box
The pulse has a deposition time which must be previously calculated.
O.1 - 1 μs
Annealing time = Pulse rate (sec) - Pulse deposition time
Input parameters of the KMC simulation are :
temperature, dose rate, dose

Multiscale approach for Continuous irradiation

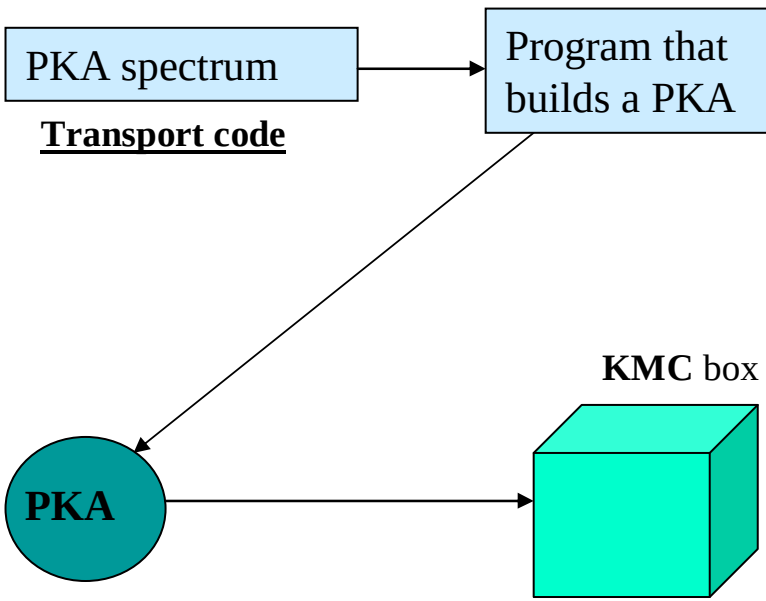

Input parameters of the KMC simulation are :

temperature, dose rate, dose

PKA introduction is constant.

Each PKA is build

according to the spectral distribution

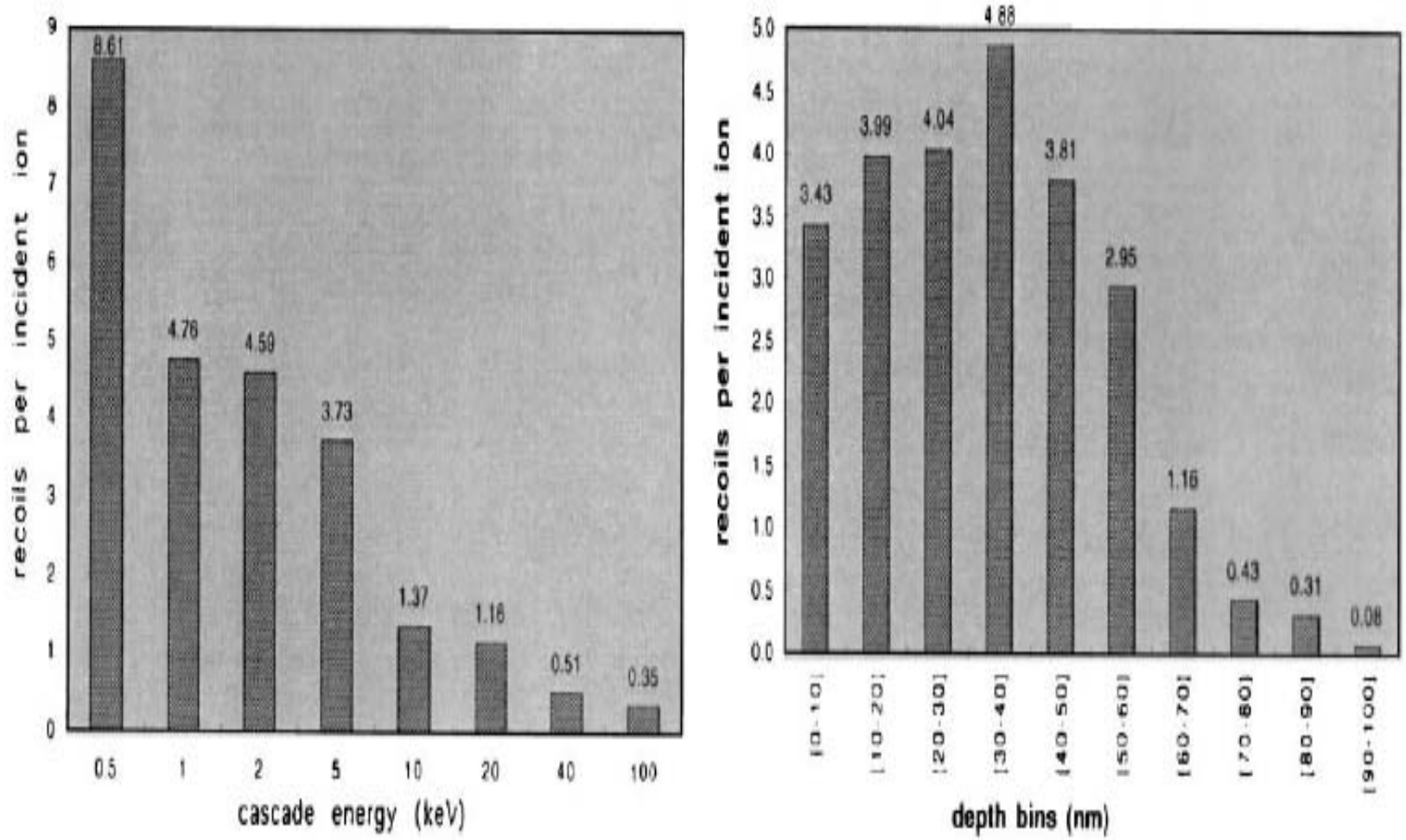

Fig. 1. Spatial and energy distributions of recoils generated by 150 keV Fe^{+} in Fe.

The simulated dose rate corresponds to 10^{15} n/cm^2/s integrated over time. The dose rate in the pulse itself is of the order of 1.4 dpa/s in Fe, and the pulse length is 1 microsecond. At 4 Hz, it results in a damage rate of 150 dpa/yr.

We should point out that the highest energy simulated by MD is 50 keV recoils of Fe in Fe, while the spectrum includes recoils of energies higher than 300 keV (after subtracting the electronic stopping). It is known that above approximately 20 keV cascades break up into subcascades of lower energy. The energy and spatial distribution of subcascades for recoils higher than 50 keV was estimated using TRIM.

Each microsecond pulse was simulated with six cascades picked at random with a probability of occurrence weighed by the modified recoil spectrum. For our KMC box of 300-nm edge length, this corresponds to instantaneous dose rates in the pulse of 1.4 dpa/s.

We simulated pulse repetition rates of 1, 10 and 100 Hz at

300 K.

At this temperature, vacancies are mobile
and small vacancy clusters dissociate.

We also simulated pulsed irradiation at 100 Hz and 620 K, well within stage V, where vacancy clusters are unstable.

For the MFE continuous irradiation, we chose a dose rate of $1.4\ 10^{-6}$ dpa/s, which is the expected in some typical MFE reactor, and a temperature of 300 K to compare with the pulsed irradiation cases.

The main **computational problem** stems from the high mobility of SIA clusters that undergo 1-D glide.

The cross-section for these clusters to participate in any reaction is rather low. Unfortunately, their low migration energy makes them a highly likely event that slows down the computation clock.

In order to speed up the simulation, we opted for the following approximation:

After the input of each cascade, a gliding direction is randomly determined for each of these 1-D migrating clusters. If they intersect any other defect in their trajectory, the reaction immediately occurs. If they do not, they are taken out of the simulation and put back in again when the next cascade arrives. Obviously, this approximation is valid only when few microstructural features are present, that is to say, at low dose.

In the plots, it is clearly seen that **the longer the time between pulses, the lower the vacancy cluster concentration but the greater their size.**

The cluster density is not appreciably different between the 1 Hz case and continuous irradiation, but the vacancy cluster size is larger for 1 Hz pulsed irradiation.

Although their integrated doses are equal (1.4 10-6 dpa/s), the annealing time between pulses is 1 s at 1 Hz, whereas the time between cascades is only 0.16 s in the MFE case.

The **interstitial cluster density at traps is completely independent of the pulse rate** and the same applies to the population of sessile interstitial clusters
(sessile interstitial clusters are formed by the intersection of two gliding SIA clusters).

For pulsed irradiation, the sequence of events is as follows. The instantaneous dose rate during the pulse is so high that nothing occurs until the pulse is over.

The annealing between pulses begins with the quick vacancy recombination with fast mobile interstitial clusters. This first stage spans over the first 0.5 s of the annealing and ends when all the SIA clusters have been trapped by impurities.

That is why the concentration of interstitial clusters shows no pulse rate dependence, because their migration is so fast that all the events which involve interstitial clusters have already taken place before the arrival of the next pulse, independently of the pulse rate.

At 300 K, the vast majority of trapped clusters are unable to overcome the detrapping barrier. From that moment until the next pulse, vacancies are free to move and cluster. Also, small vacancy clusters break up and drive cluster growth.

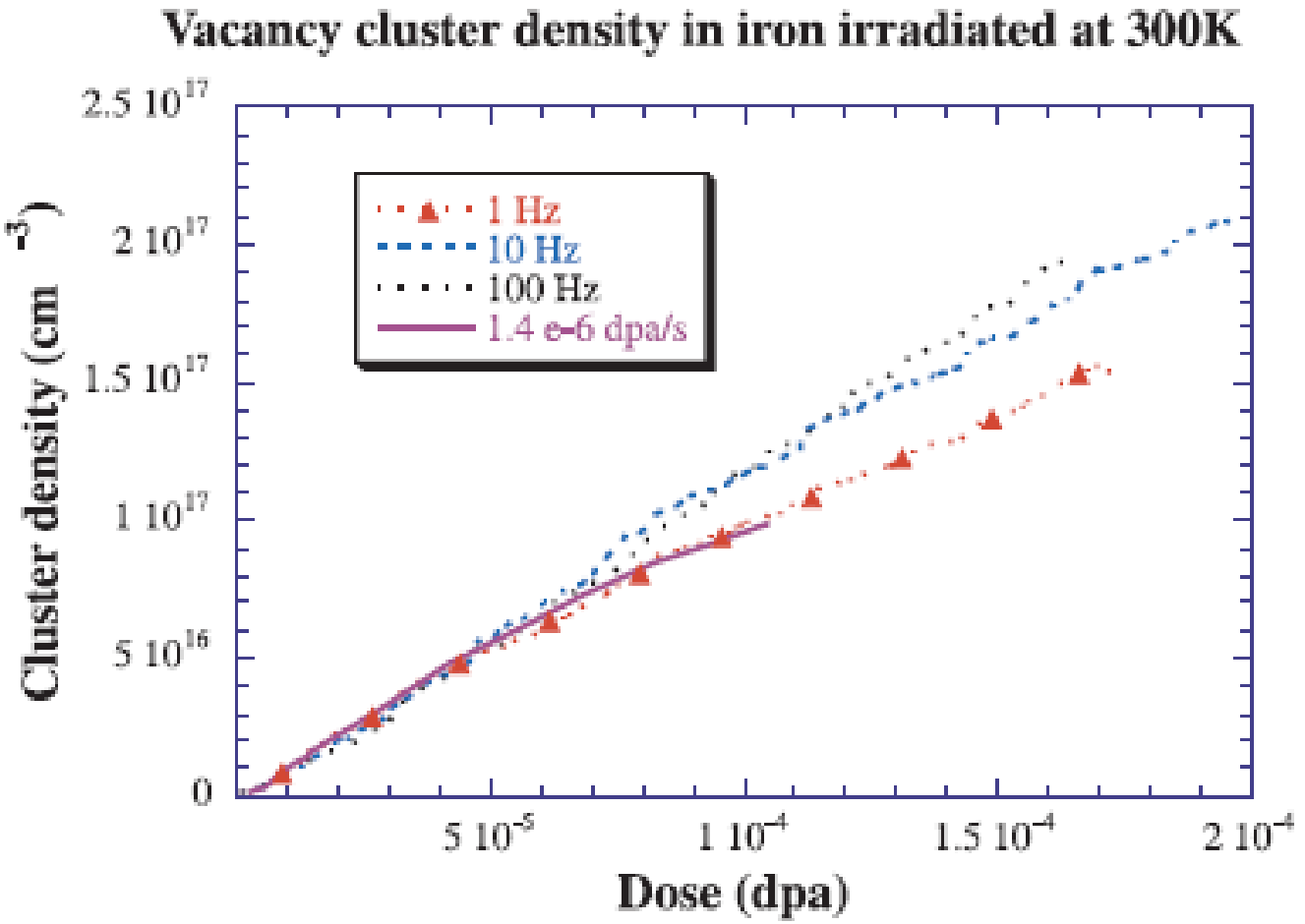

Fig. 1. Vacancy cluster density as a function of dose for 1, 10, 100 Hz pulsed irradiation and 1.4×10^{-6} dpa/s continuous irradiation at 300 K.

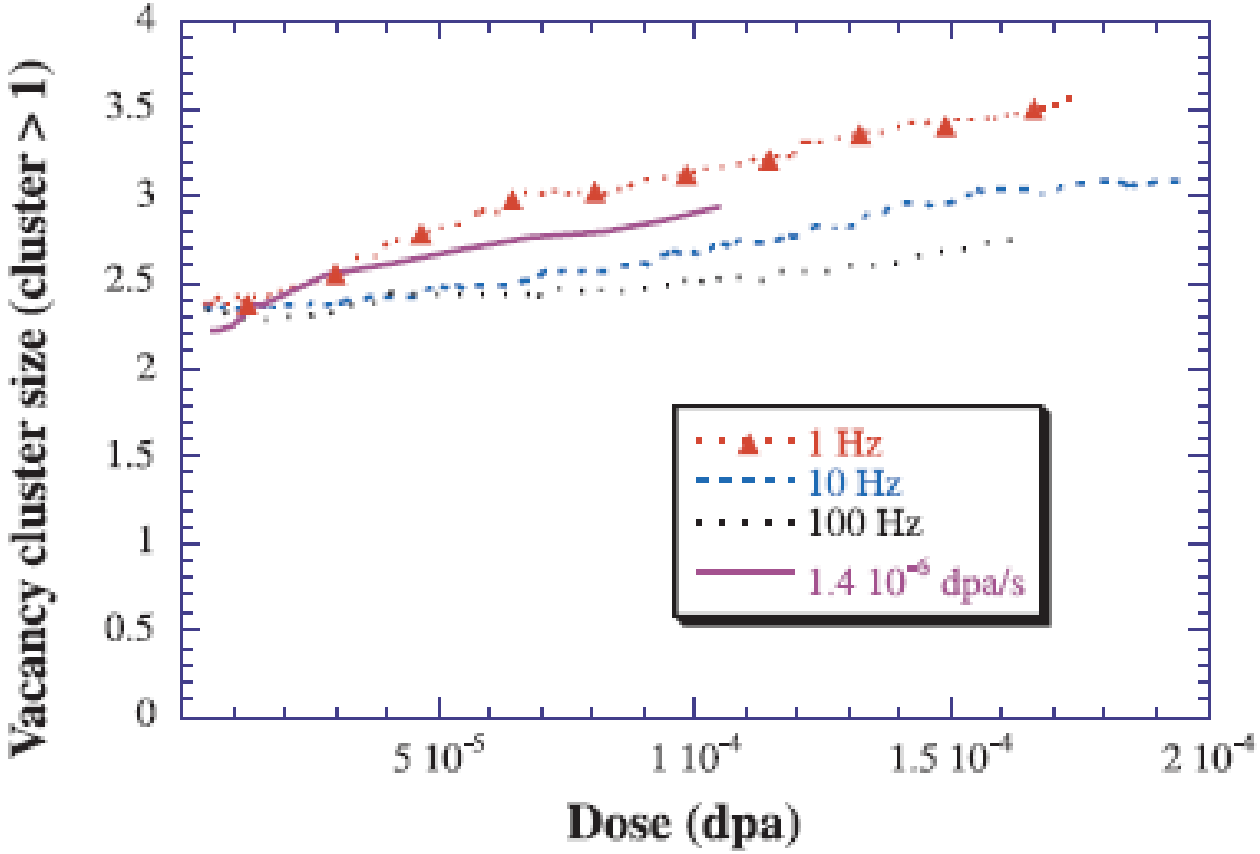

Fig. 4. Average vacancy cluster size as a function of dose for 1, 10, 100 Hz pulsed irradiation and 1.4×10^{-6} dpa/s continuous irradiation at 300 K.

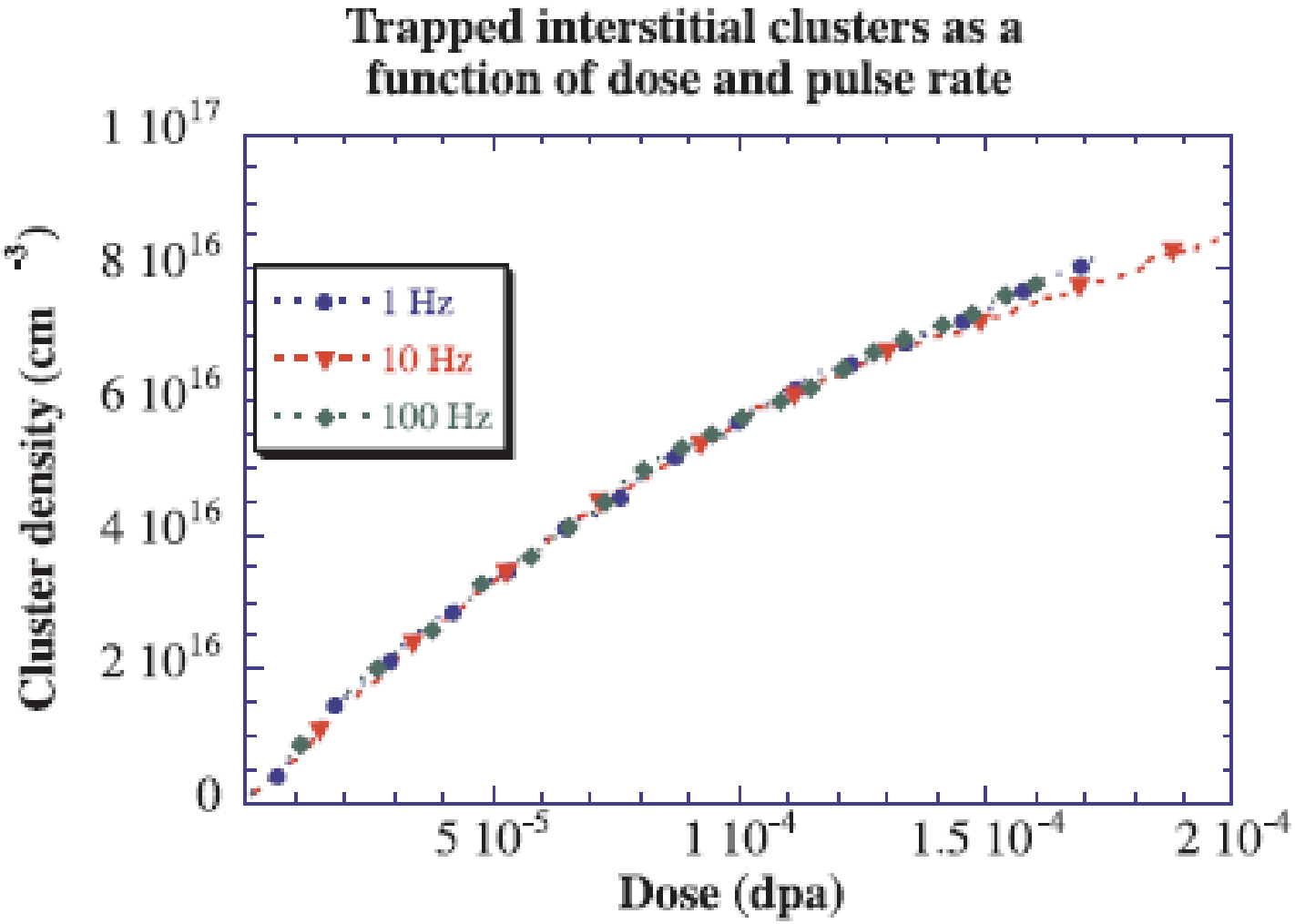

Fig. 2. Interstitial cluster density at traps as a function of dose for 1, 10, 100 Hz pulsed irradiation at 300 K.

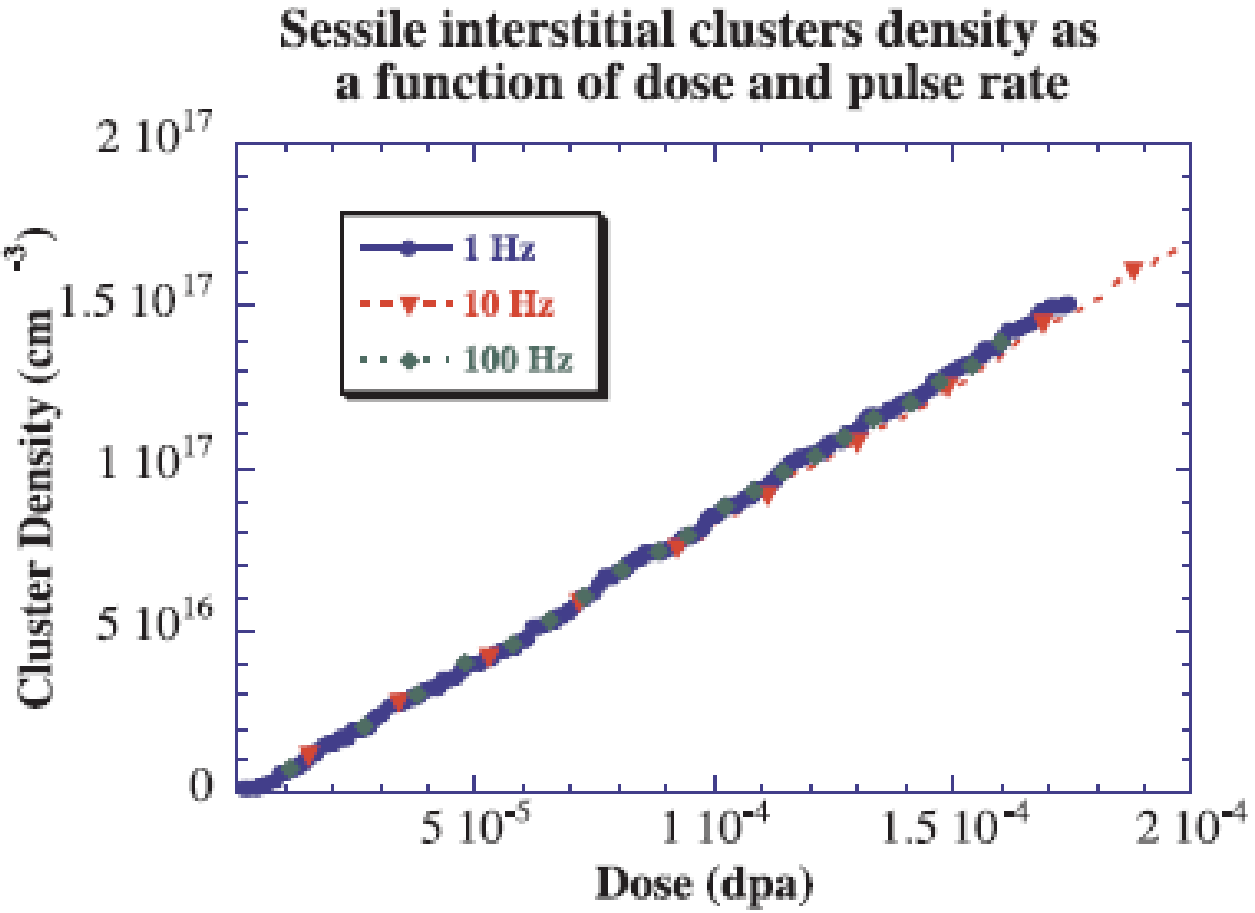

Fig. 3. Sessile interstitial clusters as a function of dose for 1, 10, 100 Hz pulsed irradiation at 300 K.

Unfortunately, our results are not directly comparable with any experiments performed in the past. Most of the experimental work on pulsed irradiation in the literature concludes that pulsed irradiation reduces the void nucleation rate and alters the void growth rate.

No helium was included as an impurity in our study, so void nucleation and growth could not be studied. However, there is a considerable amount of work on pulsed irradiation based on kinetic rate theory. In his comparison of different pulsed irradiation systems,

Ghoniem (1980) concluded that the concentration of loops was higher in pulsed systems than in continuously irradiated environments. This is in clear disagreement with our results. Nevertheless, the fast interstitial cluster migration, responsible for the independence of cluster density and pulse rate, was not contemplated in Ghoniem's study.

The temperature effect can be observed pulsed irradiation at 100 Hz.

At **620 K (Stage V), the vacancy cluster density is lower than at 300 K but their size larger.** This is a consequence of the quick coarsening process with increasing temperatures. At 620 K the minimum vacancy cluster size allowed by temperature is considerably high. Thus, **since cluster growth is faster at high temperatures, differences between pulsed and continuous irradiation are expected to be more pronounced.**

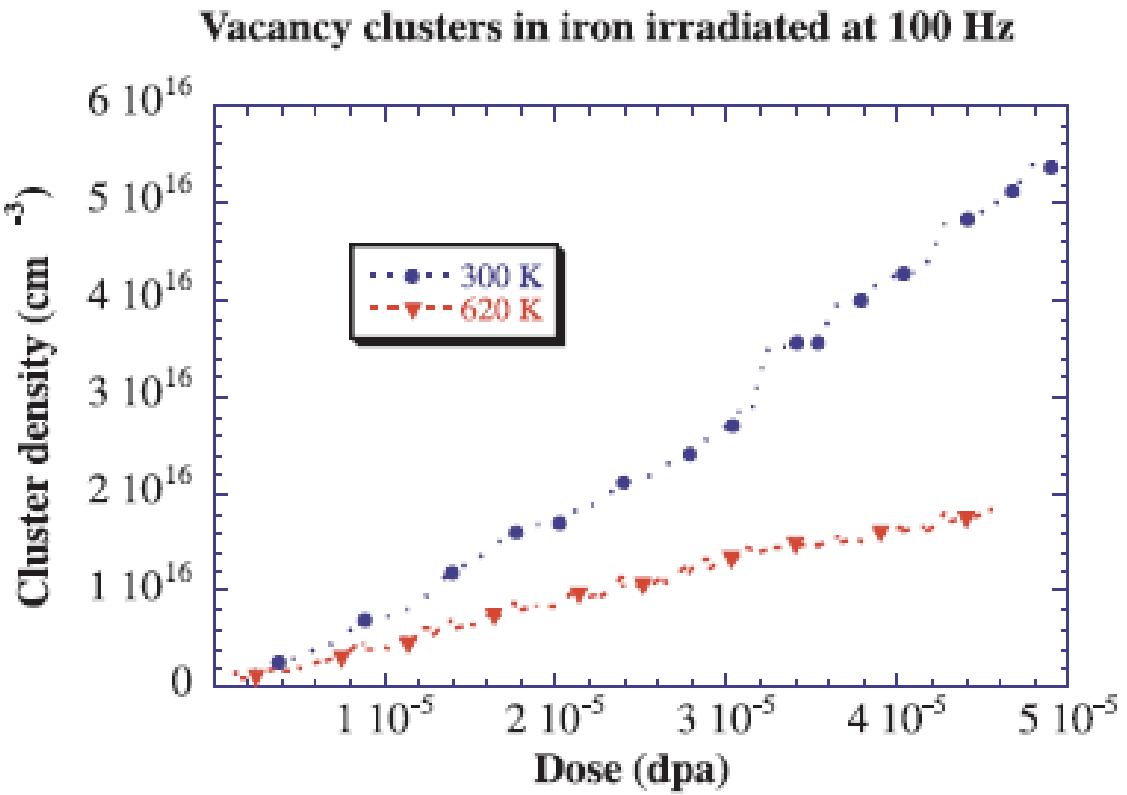

Fig. 5. Vacancy cluster density as a function of dose for 100 Hz pulsed irradiation at 300 and 620 K.

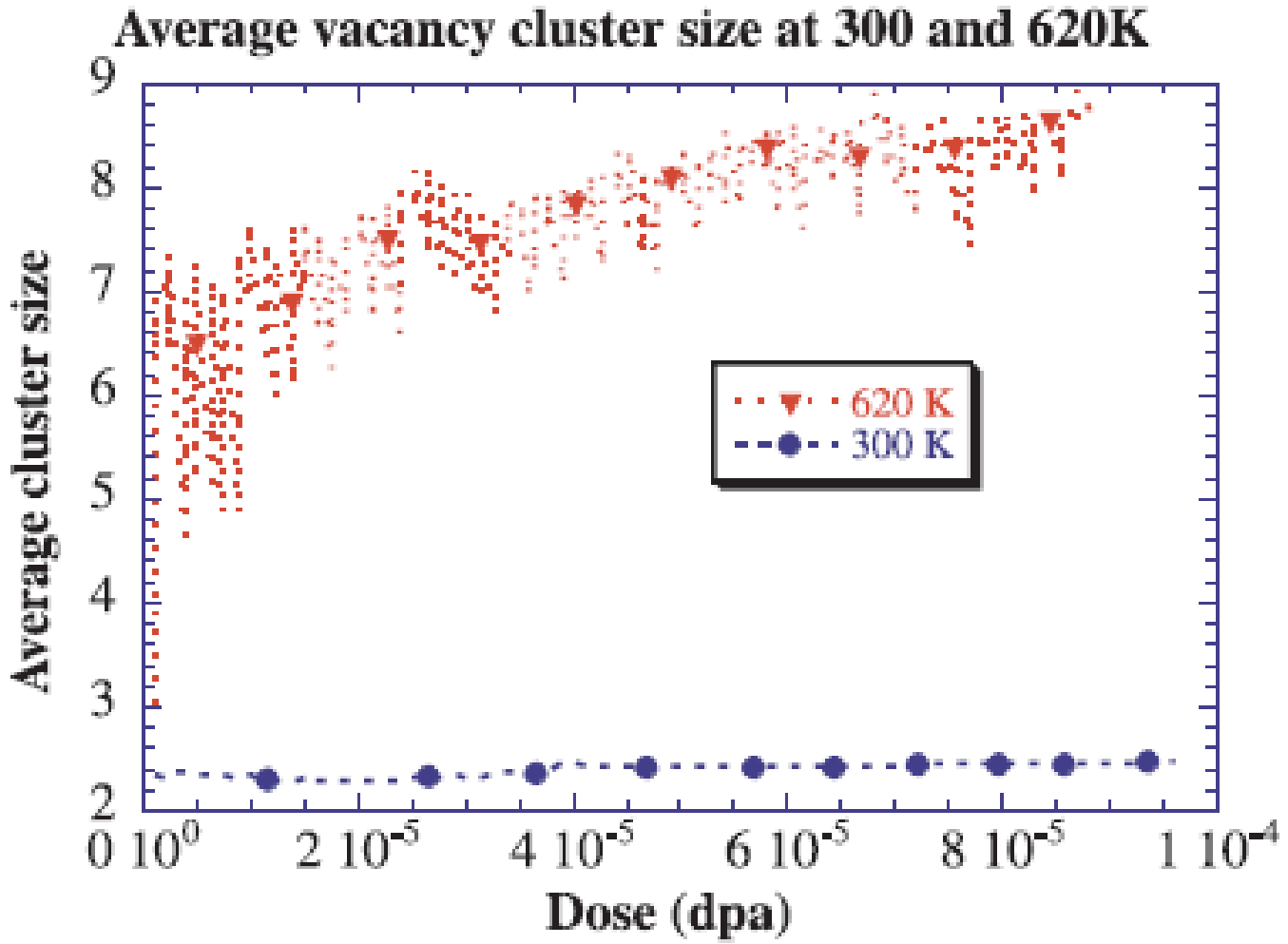

Fig. 6. Average vacancy cluster size as a function of dose for 100 Hz pulsed irradiation at 300 and 620 K.

This shows the evolution of vacancy cluster concentration during one pulse. There is, a very fast interstitial–vacancy recombination process that leads to a steep decrease in the concentration. After all the interstitials have disappeared in sinks, have interacted with impurities or have reacted with vacancies, the vacancy concentration tends to remain stable. The most probable events that can occur in this situation are di-vacancy migration, and di-vacancy splitting into two single vacancies. The results of the first event would be a decrease in vacancy cluster concentration due to the fact that it is highly probable that during migration the divacancy cluster could interact with another vacancy and form a three-vacancy cluster whose probability of splitting or diffusing is much lower.

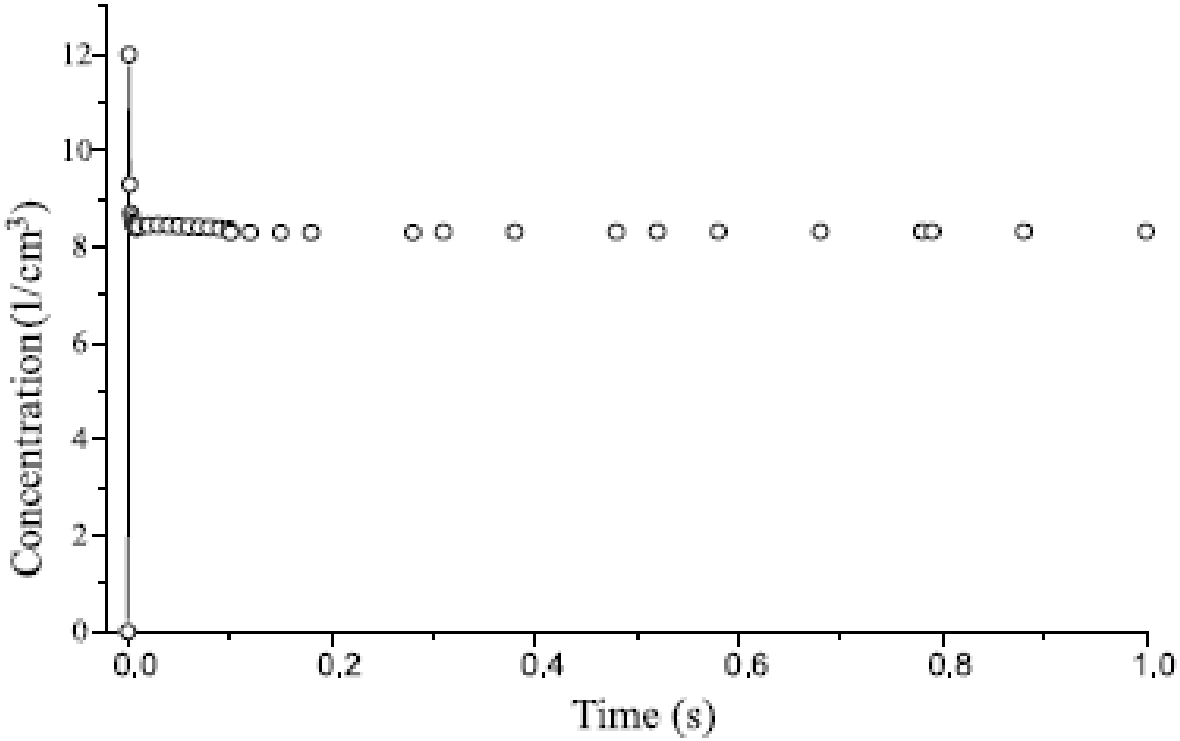

Fig. 2. Vacancy cluster concentration vs. time at 1 Hz.

The second mechanism would lead to an increase of vacancy cluster concentration. In this case the single-vacancy is not very likely to move at the temperature considered in the simulation; but again we have to consider the fact that vacancies are situated in a very small region and so the probability is not negligible for a single-vacancy, resulting from the splitting of a di-vacancy, to find another vacancy in the capture volume. **In our simulations we have noted that the vacancy cluster concentration remains basically stable and in some cases shows a little decrease during a single pulse.** The first result can be ascribable to the mechanism explained before, splitting and recombination, or simply to an immobility of the vacancies. The decrease in vacancy cluster concentration must in turn be attributed to a di-vacancy migration and final recombination with another vacancy to form a bigger cluster.

Interstitial lifetime is so short that pulse frequency plays no role in the accumulation. For this reason no differences appear in the trapped interstitial concentration. When plotting vacancy cluster accumulation versus dose no significant difference was observed between different dose rates per pulse and pulse frequencies at the accumulated dose in these simulations.

The observable differences can be attributed to a repetition rate effect, which can be summarized by saying that the more time that elapses between pulses, the more probable it is for a di-vacancy (that has the lowest migration energy) to undergo migration.

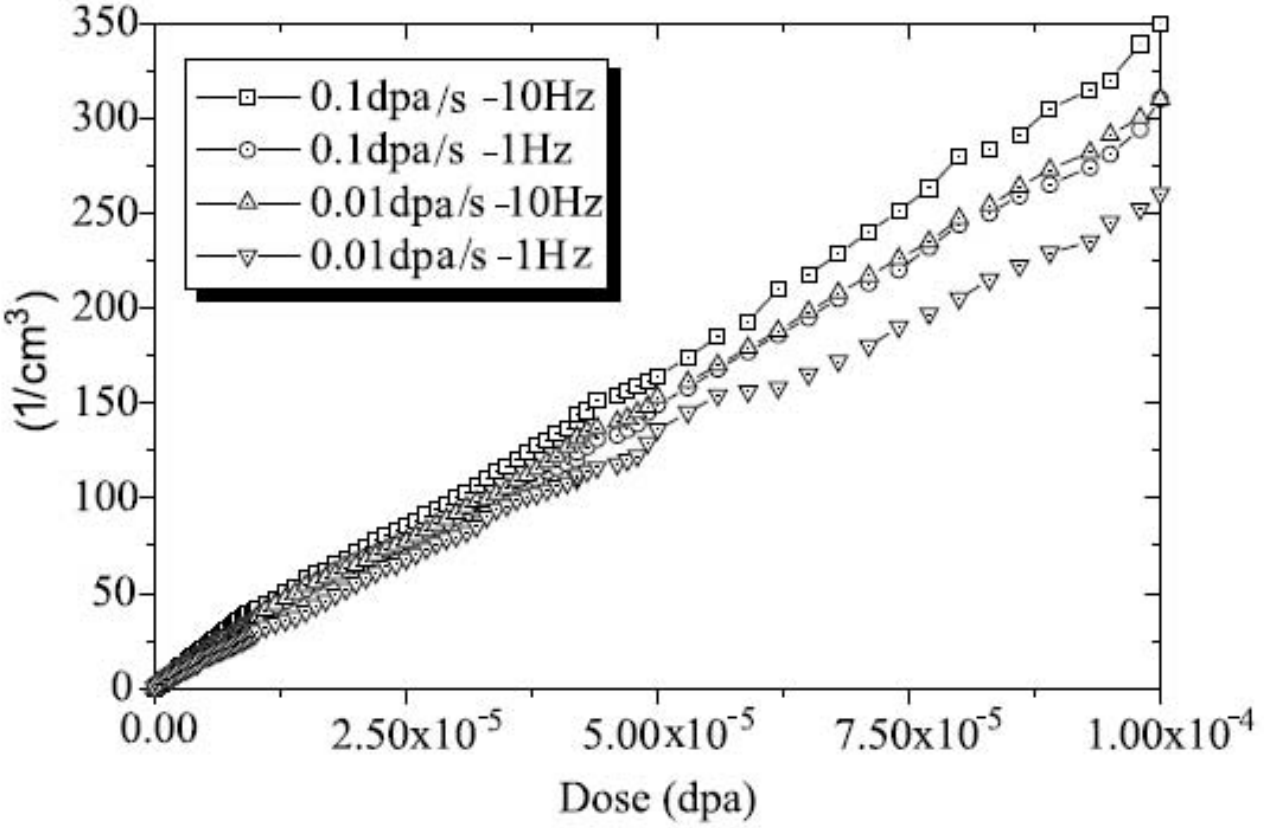

Fig. 3. Vacancy cluster concentration vs. dose.

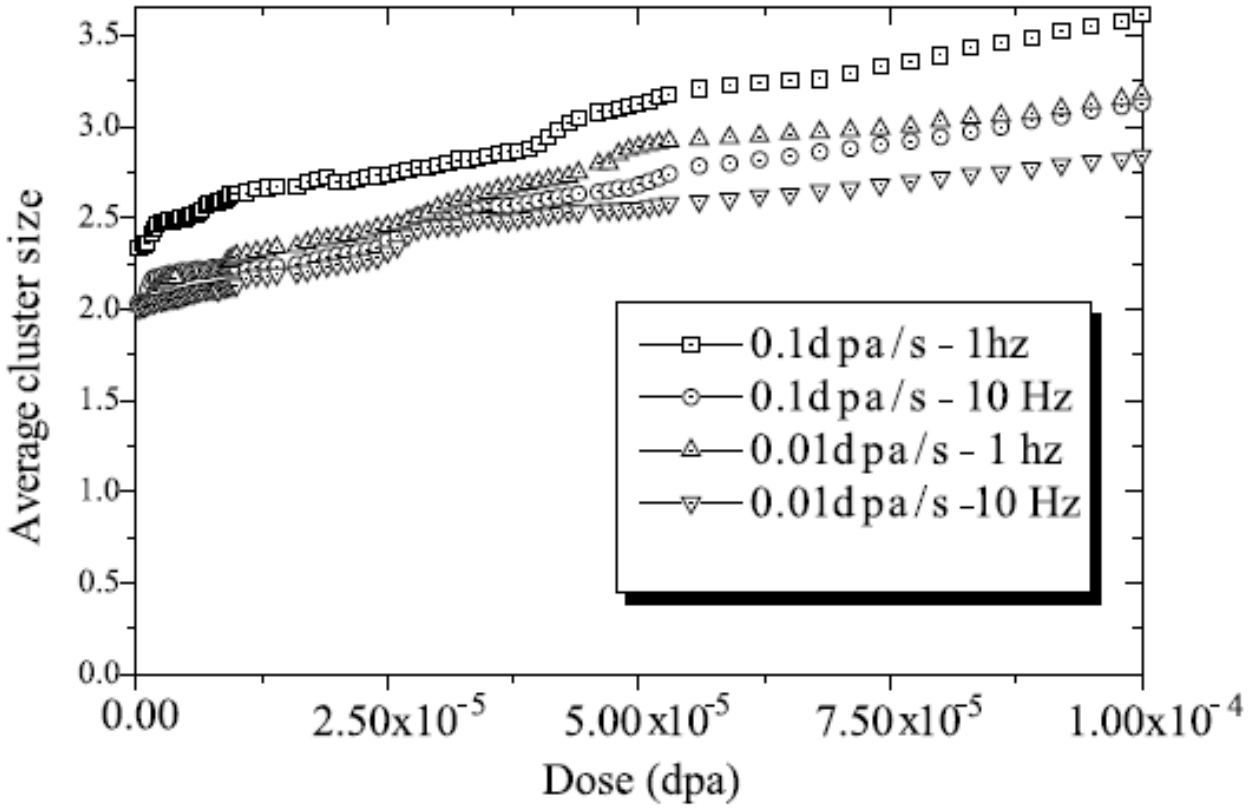

Fig. 4. Average vacancy clusters size vs. dose.

What is more likely to happen when the di-vacancy migrates is a reaction with a vacancy to form a bigger cluster, raising the average cluster size and diminishing the vacancy cluster concentration. The spatial distribution of the defects introduced in the KMC box reflects the characteristics of the collisional cascade in iron with vacancies in the core region and an interstitial shell.

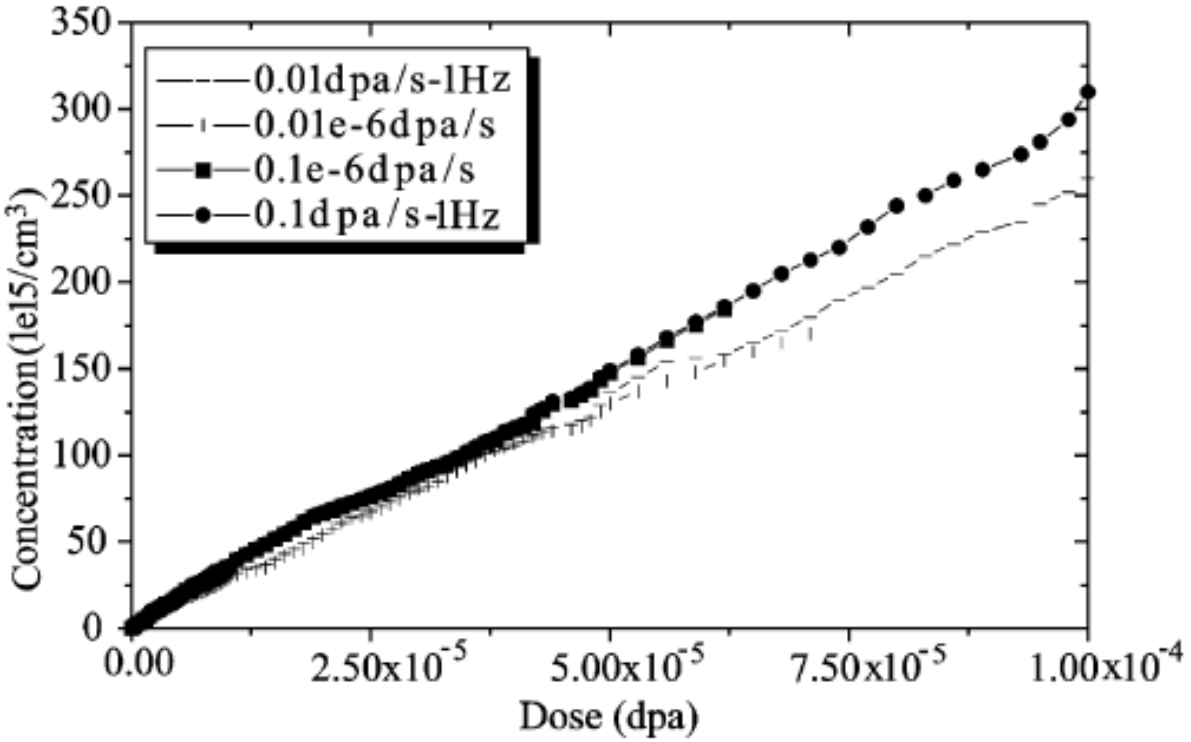

Fig. 5. Comparison between pulsed and continuous irradiation (0.1×10^{-6}–0.01×10^{-6} dpa/s).

Figure shows the comparison between pulsed and continuous irradiation. We have compared the effect of pulsed irradiation with a continuous irradiation with the same average dose rate and the results show practically identical behavior as far as vacancy cluster accumulation is concerned. This last result is coincident with the one obtained at a higher dose rate.

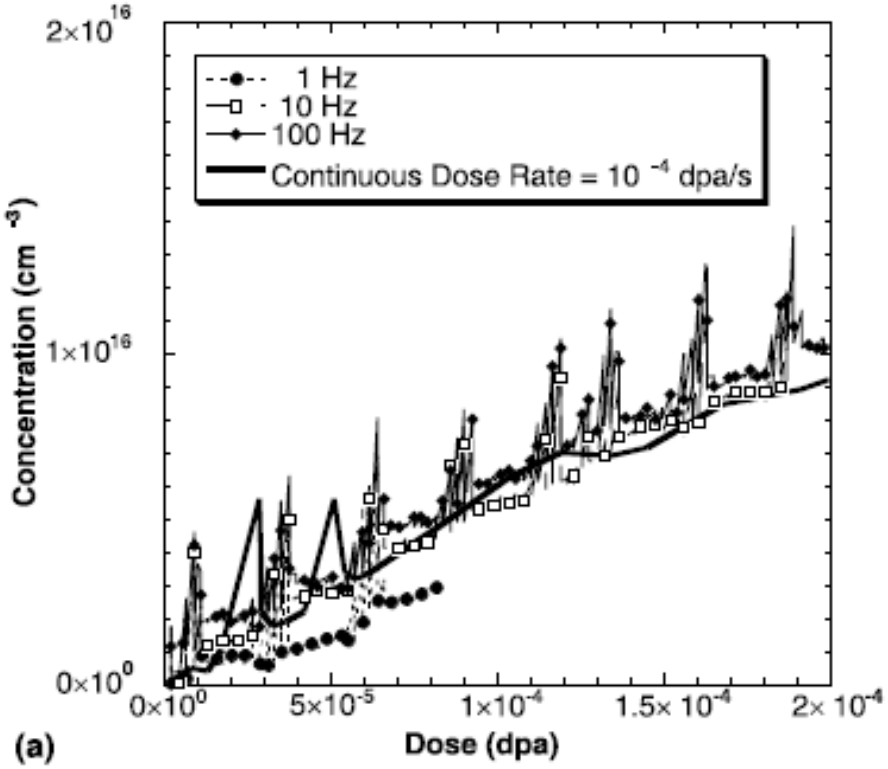

Fig. 10. Evolution of the vacancy cluster population in Cu as a function of: (a) dose at 340 K for pulse rates of 1, 10 and 100 Hz and continuous irradiation, (b) time for pulse rates of 10 and 100 Hz.

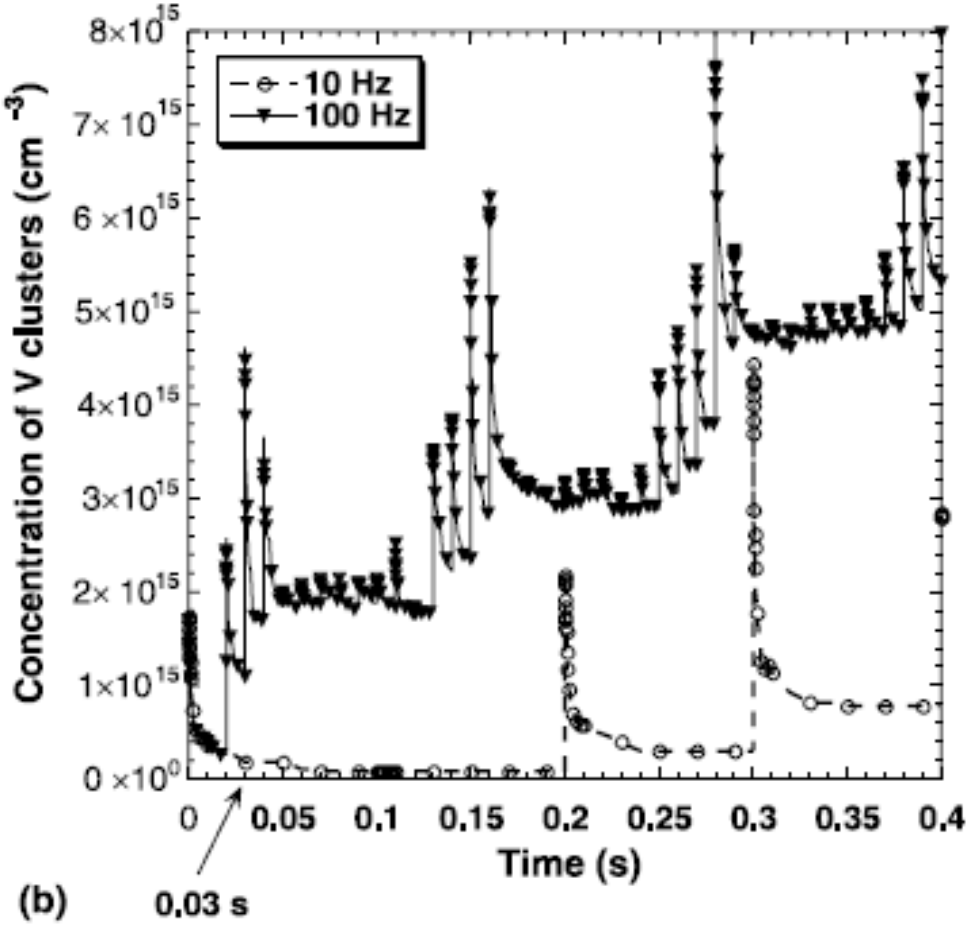

Fig. 10. Evolution of the vacancy cluster population in Cu as a function of: (a) dose at 340 K for pulse rates of 1, 10 and 100 Hz and continuous irradiation, (b) time for pulse rates of 10 and 100 Hz.

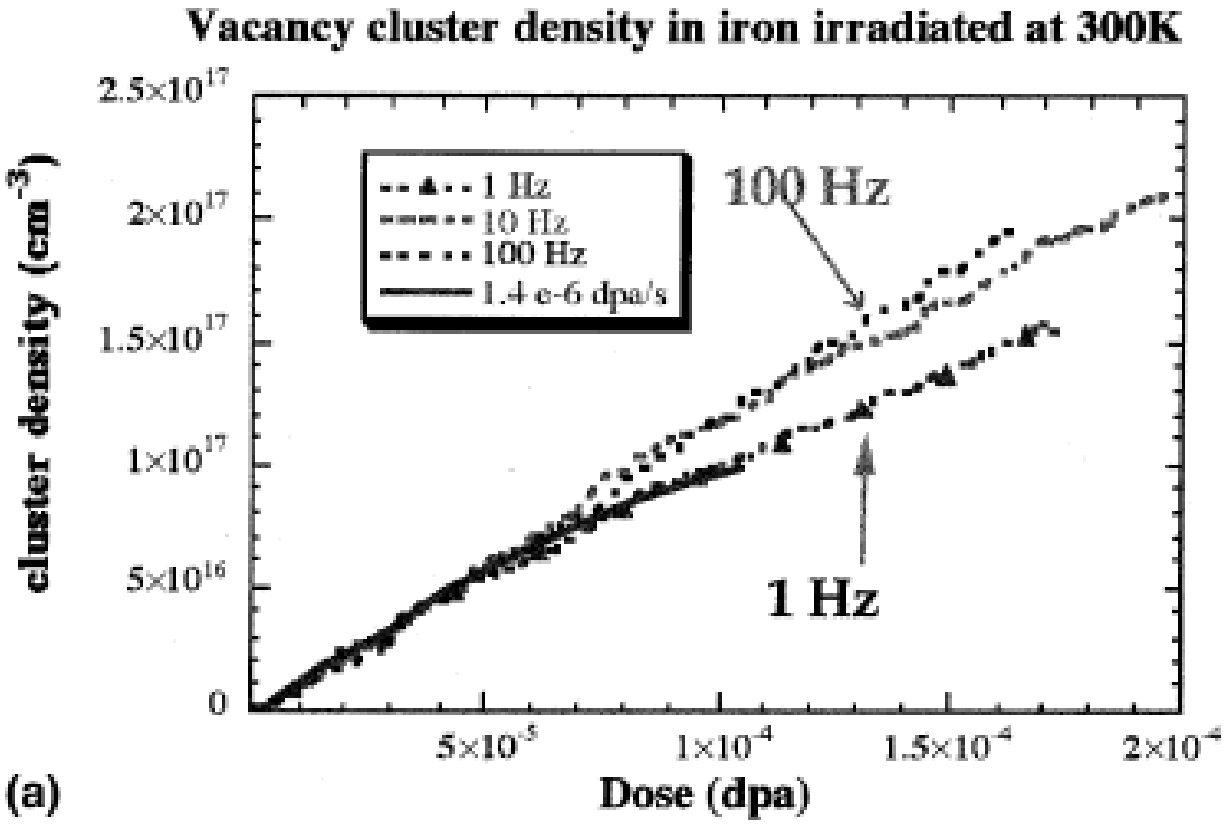

Fig. 11. (a) Evolution of the vacancy cluster density in Fe as a function of dose for pulse rates of 1, 10 and 100 Hz and continuous irradiation, (b) as a function of irradiation time for a 1 Hz pulse.

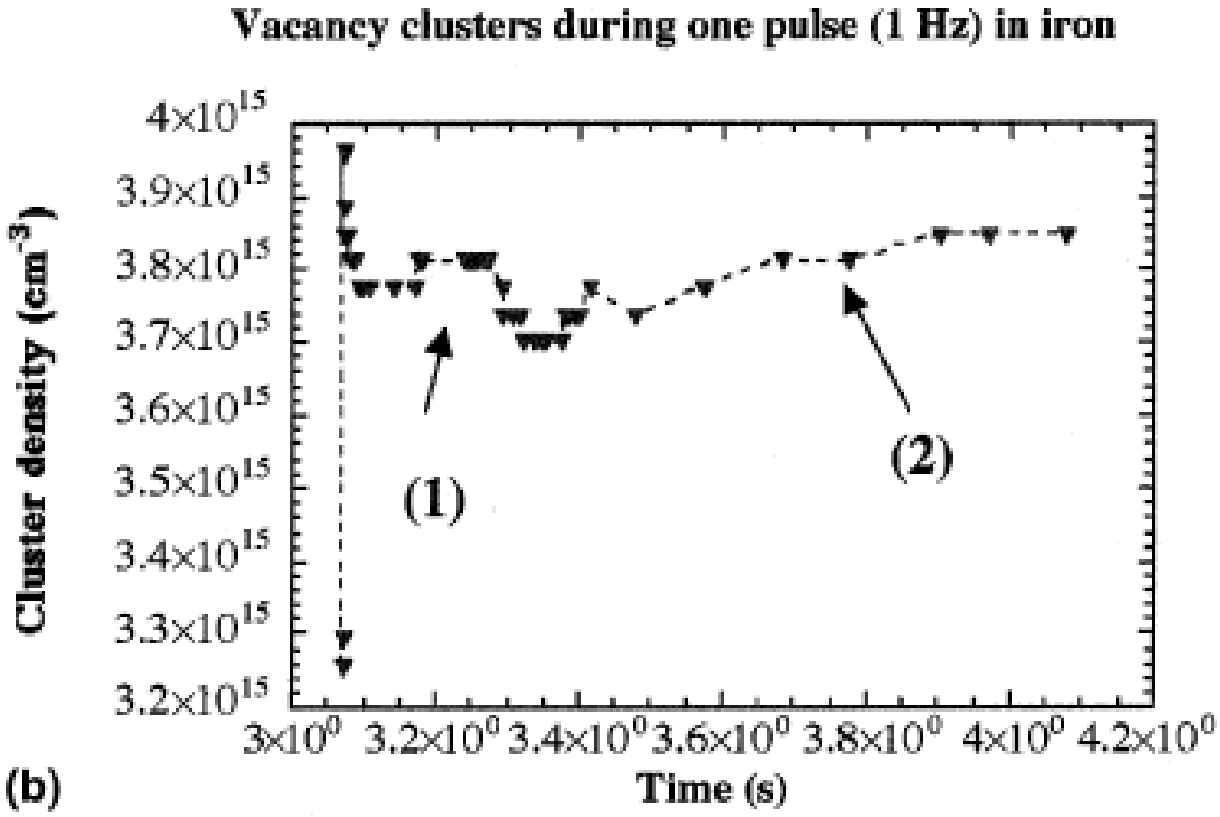

Fig. 11. (a) Evolution of the vacancy cluster density in Fe as a function of dose for pulse rates of 1, 10 and 100 Hz and continuous irradiation, (b) as a function of irradiation time for a 1 Hz pulse.